RSC Advances

This article can be cited before page numbers have been issued, to do this please use: J. Peng, H. Yang, Z. Wei and C. Guo, *RSC Adv.*, 2015, DOI: 10.1039/C5RA08237D.

ROYAL SOCIETY OF CHEMISTRY

www.rsc.org/advances

Dynamic Article Links ►
View Article Online
DOI: 10.1039/C5RA08237D

Cite this: DOI: 10.1039/c0xx00000x

www.rsc.org/xxxxxx

ARTICLE TYPE

Metal Complexes Bearing 2-(Imidazol-2-yl)phenol Ligands: Synthesis, Characterization and Catalytic Performance in the Fixation of Carbon Dioxide with Epoxides

Jing Peng[a,b], Hai-Jian Yang*,[b] Zidong Wei[a], Cun-Yue Guo*,[c]

Received (in XXX, XXX) Xth XXXXXXXXX 2015, Accepted Xth XXXXXXXXX 2015
DOI: 10.1039/b000000x

A series of metal complexes bearing 2-(imidazol-2-yl)phenol ligands (Zn, Cu, Ni, Co, Pb) were synthesized and their structures were characterized by IR, NMR, elemental analysis and X-ray. The catalytical activities of all complexes for the coupling reaction of CO_2 and epoxide were then detected. The activity influence factors, such as temperature, time, pressure, substituents of ligands and metal centre, were systematically investigated. All these complexes were efficient to catalyze the coupling of CO_2 and epoxide to generate cyclic carbonate in perfect yields (>90%) and selectivities (>99%) under optimized conditions of (2 MPa, 5 h, 110 °C) without any organic solvents. A 99.7% yield and >99% selectivity for propylene carbonate (PC) were obtained with C_7/n-Bu_4NI as catalyst system under the optimized conditions. The catalysts were also proved to be applicable to other terminal epoxides. It is worthy noted that the Pb(II) complex was firstly used to catalyze the coupling reaction of epoxides with carbon dioxide. Moreover, these metal catalysts were recyclable with only minor losses in catalytic activity after simple separation. Finally, a plausible mechanism was given.

1. Introduction

As an alternative, sustainable feedstock for the chemical industry, the conversion of CO_2 into useful chemicals has become a public concern due to the global warming and severe energy crisis.[1-4] The coupling reaction of CO_2 with epoxides to produce either polycarbonates[5-7] or cyclic carbonates[8-11] is considered to be one of the promising routes for CO_2 utilization. The cyclic carbonates, especially five-membered cyclic carbonates, are one kind of CO_2 fixation products and widely used as monomer for polymer synthesis, aprotic solvents, electrolytes for lithium-ion batteries, and as intermediates in the manufacture of fine chemicals.[12-14] This approach is 100% atom economical and benefits from eliminating phosgene as a reagent.

Recently, numerous homogeneous and heterogeneous catalysts have been used for the synthesis of the cyclic carbonates. Homogeneous catalysts include salen, porphyrin, phthalocyanine and other complexes of the main group and transition metals,[15-18] quaternary ammonium salts,[19] ionic liquids,[20,21], polyoxometalates[22], Lewis acids or bases[23-25] and so on. Some heterogeneous catalysts[26] also have been explored for the cycloaddition of CO_2 to epoxides, such as metal oxides,[27] immobilized complexes or ionic liquids,[28-33] titanosilicates,[34] and zeolites.[35] There are also few examples of the use of the metal–organic frameworks (MOFs).[36-38] Among these catalyst systems, metal complexes have been of significant interest due to their easy synthesis and excellent stability against moisture and air.[39-43] Nevertheless, although the advances are significant, most suffer from long reaction time[39,40] and the need for toxic co-solvent.[41-43] Therefore, developing stable, efficient and solventless catalytic system for the synthesis of cyclic carbonate is still highly required. Herein, we reported the synthesis and characterization of a series of metal complexes bearing 2-(imidazol-2-yl)phenol ligands, which were proven to be efficient and recyclable catalysts for the reaction of various epoxides with CO_2 to selectively yield cyclic carbonates under mild conditions without any organic solvents. The catalytic performance has been systematically investigated, and the optimization of the catalytic system to produce cyclic carbonates with maximal yields was performed. The recyclability of the catalysts was also been detected. Furthermore, a proposed mechanism was given. To the best of our knowledge, the Pb(II) chelate complex was firstly used to catalyze the coupling reaction of epoxides with carbon dioxide in good catalytic activity and high selectivity.

2. Experimental section

2.1. Chemicals and analytical methods

The detailed information of the materials used in present work is listed in Table S1 (see supporting information). The epoxides were distilled from CaH_2.

NMR spectra were recorded on a Bruker Al-400 MHz instrument using TMS as an internal standard. IR spectra were recorded on a Perkin-Elmer 2000 FT-IR spectrometer. Elemental analysis was conducted on a PE 2400 series II CHNS/O elemental analyzer. Melting point was obtained from X-4-type digital micro-melting point apparatus. X-ray diffraction studies

View Article Online
DOI: 10.1039/C5RA08237D

were performed on a Bruker-APEX diffractometer equipped with a CCD area detector, MoKa-radiation (λ= 0.71073 Å), and a graphite monochromator. Elemental analyses were performed on a Flash EA 1112 microanalyzer. IR spectra were recorded on a Nicolet 6700 FT-IR spectrometer as KBr discs in the range of 4000-600 cm^{-1}.

2.2. Synthesis of ligands L_1–L_9

The synthesis of ligands L_1–L_9 followed the general procedure shown in Scheme 1.[44] A mixture of salicylaldehyde or corresponding salicylaldehyde derivatives (9.51 mmol), benzil (9.51 mmol), and ammonium acetate (20 equivalent) were refluxed for 2 h in glacial acetic acid (30 mL) under N_2 to form a precipitate. An excess of de-ionised water was added to complete the precipitation. The crude product was collected by filtration, washed with water, and dried by suction. The resulting solid was dissolved in CH_2Cl_2 and dried over $MgSO_4$. The solution was filtered and the solvent was evaporated from the filtrate to produce a powder. After recrystallization from CH_2Cl_2–pentane, a crystalline solid was obtained.

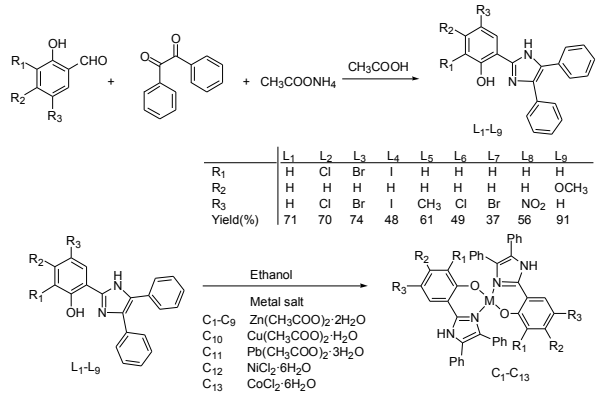

	L_1	L_2	L_3	L_4	L_5	L_6	L_7	L_8	L_9
R_1	H	Cl	Br	I	H	H	H	H	H
R_2	H	H	H	H	H	H	H	H	OCH_3
R_3	H	Cl	Br	I	CH_3	Cl	Br	NO_2	H
Yield(%)	71	70	74	48	61	49	37	56	91

	C_1	C_2	C_3	C_4	C_5	C_6	C_7	C_8	C_9	C_{10}	C_{11}	C_{12}	C_{13}
M	Zn	Zn	Zn	Zn	Zn	Zn	Zn	Zn	Zn	Cu	Pb	Ni	Co
R_1	H	Cl	Br	I	H	H	H	H	H	H	H	H	H
R_2	H	H	H	H	H	H	H	H	OCH_3	H	H	H	H
R_3	H	Cl	Br	I	CH_3	Cl	Br	NO_2	H	H	H	H	H
Yield(%)	96	99	98	92	82	93	86	93	88	99	49	12	26

Scheme 1 Synthesis of ligands L_1-L_9 and complexes C_1-C_{13}. The molecular structures of ligands are only different by substituents.

L_1 (2-(4,5-diphenyl-1H-imidazol-2-yl)phenol): 71% yield. Mp. 202 – 204 °C. Selected IR peaks (KBr, cm^{-1}): ν 3208, 3058, 1598, 1539, 1135, 1074, 695. ^{1}H NMR (400 MHz, DMSO) δ 13.04 (s, 1H), 12.96 (s, 1H), 8.05 (d, J = 7.6 Hz, 1H), 7.59 – 7.37 (m, 7H), 7.37 – 7.19 (m, 4H), 6.97 (m, 2H). ^{13}C NMR (101 MHz, DMSO) δ 157.18, 146.33, 134.64, 130.76, 128.98, 128.80, 127.78, 127.54, 127.27, 119.33, 117.30, 113.36. Anal. Calcd for $C_{21}H_{16}N_2O$: C, 80.77; H, 5.13; N, 8.97%. Found: C, 81.70; H, 5.15; N, 8.95%.

L_2 (2,4-dichloro-6-(4,5-diphenyl-1H-imidazol-2-yl)phenol): 70% yield. Mp. 209 – 210 °C. Selected IR peaks (KBr, cm^{-1}): ν 3315, 3063, 1463, 1373, 1262, 1079, 696. ^{1}H NMR (400 MHz, DMSO) δ 8.18 (d, J = 2.5 Hz, 2H), 7.56 (m, 8H), 7.44 (s, 4H). ^{13}C NMR (101 MHz, DMSO) δ 156.13, 146.57, 134.24, 131.37, 129.20, 129.11, 127.95, 127.88, 127.31, 125.63, 125.45, 118.29. Anal. Calcd for $C_{21}H_{14}N_2OCl_2$: C, 66.14; H, 3.67; N, 7.35%. Found: C, 66.17; H, 3.67; N, 7.34%.

L_3 (2,4-dibromo-6-(4,5-diphenyl-1H-imidazol-2-yl)phenol): 74% yield. Mp. 193 – 195 °C. Selected IR peaks (KBr, cm^{-1}): ν 3321, 3069, 1450, 1367, 1259, 1077, 697. 1H NMR (400 MHz, DMSO) δ 8.34 (d, J = 2.3 Hz, 1H), 7.79 (d, J = 2.3 Hz, 1H), 7.54 (d, J = 7.0 Hz, 5H), 7.44 (s, 7H). ^{13}C NMR (101 MHz, DMSO) δ 155.88, 146.49, 137.37, 134.63, 134.28, 129.97, 129.91, 128.12, 127.70, 122.95, 118.37, 116.64. Anal. Calcd for $C_{21}H_{14}N_2OBr_2$: C, 53.62; H, 2.98; N, 5.96%. Found: C, 53.65; H, 3.01; N, 5.97%.

L_4 (2,4-diiodo-6-(4,5-diphenyl-1H-imidazol-2-yl)phenol): 48% yield. Mp. 203 – 205 °C. Selected IR peaks (KBr, cm^{-1}): ν 3331, 3064, 1443, 1378, 1257, 1001, 697. ^{1}H NMR (400 MHz, DMSO) δ 8.45 (d, J = 2.0 Hz, 1H), 8.02 (d, J = 2.0 Hz, 1H), 7.54 (d, J = 7.1 Hz, 5H), 7.46 – 7.41 (m, 7H). ^{13}C NMR (101 MHz, DMSO) δ 163.91, 147.89, 145.66, 137.49, 133.28, 129.37, 129.15, 128.73, 127. 38, 121.57, 99.99, 99.84. Anal. Calcd for $C_{21}H_{14}N_2OI_2$: C, 44.68; H, 2.48; N, 4.96%. Found: C, 44.64; H, 2.50; N, 4.94%.

L_5 (4-methyl-2-(4,5-diphenyl-1H-imidazol-2-yl)phenol): 61% yield. Mp. 190 – 192 °C. Selected IR peaks (KBr, cm^{-1}): ν 3280, 3035, 1505, 1378, 1249, 1073, 695. ^{1}H NMR (400 MHz, DMSO) δ 12.97 (s, 1H), 12.67 (s, 1H), 7.89 (d, J = 1.4 Hz, 1H), 7.58 – 7.23 (m, 10H), 7.09 (m, 1H), 6.88 (d, J = 8.3 Hz, 1H), 2.30 (s, 3H). ^{13}C NMR (101 MHz, DMSO) δ 155.06, 146.45, 134.70, 131.17, 130.79, 129.17, 128.95, 128.70, 127.81, 125.52, 117.07, 112.98, 20.69. Anal. Calcd for $C_{22}H_{18}N_2O$: C, 80.98; H, 5.52; N, 8.59%. Found: C, 80.95; H, 5.49; N, 8.58%.

L_6 (4-chloro-2-(4,5-diphenyl-1H-imidazol-2-yl)phenol): 49% yield. Mp. 198 – 200 °C. Selected IR peaks (KBr, cm^{-1}): ν 3224, 2370, 1489, 1374, 1254, 1077, 696. ^{1}H NMR (400 MHz, DMSO) δ 13.14 (s, 1H), 13.05 (s, 1H), 8.18 (d, J = 2.6 Hz, 1H), 7.59 – 7.43 (m, 7H), 7.33 (m, 4H), 7.02 (d, J = 8.8 Hz, 1H). ^{13}C NMR (101 MHz, DMSO) δ 153.14, 147.07, 133.61, 130.25, 129.71, 129.53, 128.96, 128.83, 127.75, 127.40, 120.11, 117.93. Anal. Calcd for $C_{21}H_{15}N_2OCl$: C, 72.73; H, 4.33; N, 8.08%. Found: C, 72.77; H, 4.35; N, 8.08%.

L_7 (4-bromo-2-(4,5-diphenyl-1H-imidazol-2-yl)phenol): 37% yield. Mp. 181 – 183 °C. Selected IR peaks (KBr, cm^{-1}): ν 3207, 2370, 1485, 1369, 1253, 1075, 696. ^{1}H NMR (400 MHz, DMSO) δ 13.14 (s, 1H), 13.08 (s, 1H), 8.31 (d, J = 2.4 Hz, 1H), 7.53 (s, 5H), 7.46 – 7.34 (m, 5H), 6.97 (d, J = 8.8 Hz, 2H). ^{13}C NMR (101 MHz, DMSO) δ 154.28, 147.95, 134.77, 133.82, 133.34, 129.61, 129.07, 128.93, 127.81, 120.89, 119.02, 116.28. Anal. Calcd for $C_{21}H_{15}N_2OBr$: C, 64.85; H, 3.84; N, 7.16%. Found: C, 64.85; H, 3.85; N, 7.19%.

L_8 (4-nitro-2-(4,5-diphenyl-1H-imidazol-2-yl)phenol): 56% yield. Mp. 250 – 252 °C. Selected IR peaks (KBr, cm^{-1}): ν 3295, 2367, 1486, 1334, 1296, 1130, 696. ^{1}H NMR (400 MHz, DMSO) δ 14.12 – 13.82 (m, 2H), 9.16 (d, J = 2.7 Hz, 1H), 8.18 (m, 1H), 7.61 – 7.49 (m, 4H), 7.42 (m, 6H), 7.19 (d, J = 9.1 Hz, 1H). ^{13}C NMR (101 MHz, DMSO) δ 158.32, 144.51, 138.79, 130.03, 129.55, 129.31, 128.47, 128.22, 124.92, 123.76, 118.23, 99.99. Anal. Calcd for $C_{21}H_{15}N_3O_2$: C, 73.90; H, 4.40; N, 12.32%. Found: C, 73.86; H, 4.42; N, 12.34%.

L_9 (5-methoxy-2-(4,5-diphenyl-1H-imidazol-2-yl)phenol): 91% yield. Mp. 220 – 221 °C. Selected IR peaks (KBr, cm^{-1}): ν 3225, 3061, 2939, 1604, 1445, 1268, 1201, 1075, 696. ^{1}H NMR (400 MHz, DMSO) δ 13.11 (s, 1H), 12.84 (s, 1H), 7.95 (d, J = 8.4 Hz, 1H), 7.48 (m, 7H), 7.31 (m, 3H), 6.60 – 6.52 (m, 2H), 3.79 (s, 3H). ^{13}C NMR (101 MHz, DMSO) δ 162.03, 156.19, 146.97, 132.92, 129.37, 129.13, 128.91, 128.32, 127.46, 110.98, 108.47,

View Article Online
DOI: 10.1039/C5RA08237D

102.95, 54.73. Anal. Calcd for $C_{22}H_{18}N_2O_2$: C, 77.19; H, 5.26; N, 8.19%. Found: C, 77.15; H, 5.30; N, 8.16%.

2.3. Synthesis of complexes C_1–C_{13}

The synthesis of complexes C_1–C_{13} followed the general procedure shown in Scheme 1.[44] Ligands L_1–L_9 (12.50 mmol) and corresponding metal salts (6.30 mmol) were dissolved in 50 mL of ethanol and refluxed at 70 °C for 3 h. The resulting precipitate was filtered, washed with a few milliliters of ethanol, and dried to obtain complexes C_1–C_{13}.

C_1 (bis(2-(4,5-diphenyl-1H-imidazol-2-yl)phenoxy)zinc) **:** 96% yield. Mp. 336 – 338 oC. Selected IR peaks (KBr, cm^{-1}): *v* 3414, 3057, 1604, 1534, 1481, 1312, 1260, 697. 1H NMR (400 MHz, DMSO) δ 12.62 (s, 2H), 7.76 (d, J = 6.3 Hz, 2H), 7.32 (m, 10H), 7.16 (t, J = 7.8 Hz, 2H), 7.12 – 6.92 (m, 6H), 6.84 (t, J = 7.7 Hz, 4H), 6.75 (d, J = 8.3 Hz, 2H), 6.55 (t, J = 6.8 Hz, 2H). 13C NMR (101 MHz, DMSO) δ 156.10, 136.93, 133.24, 130.79, 129.76, 129.48, 128.92, 128.74, 127.68, 121.86, 119.05, 116.65, 58.23. Anal. Calcd for $C_{42}H_{30}N_4O_2Zn$•$COOCH_3$: C, 70.78; H, 4.42; N, 7.51%. Found: C, 70.75; H, 4.43; N, 7.54%.

C_2 (bis(2,4-dichloro-6-(4,5-diphenyl-1H-imidazol-2-yl)phenoxy)zinc): 99% yield. Mp. 340 – 342 °C. Selected IR peaks (KBr, cm^{-1}): *v* 3414, 3180, 1599, 1529, 1467, 1392, 1247, 698. ^{1}H NMR (400 MHz, DMSO) *δ* 12.98 (s, 2H), 10.29 (d, 4H), 7.29 – 7.89 (m, 14H), 6.86 – 7.06 (m, 6H). ^{13}C NMR (101 MHz, DMSO) *δ* 154.63, 135.86, 133.81, 131.02, 129.74, 129.29, 128.85, 128.82, 127.39, 126.83, 126.21, 121.43, 53.97. Anal. Calcd for $C_{42}H_{26}N_4O_2Cl_4Zn$•$COOCH_3$: C, 59.73; H, 3.28; N, 6.33%. Found: C, 59.71; H, 3.30; N, 6.34%.

C_3 (bis(2,4-dibromo-6-(4,5-diphenyl-1H-imidazol-2-yl)phenoxy)zinc): 98% yield. Mp. 335 – 337 °C. Selected IR peaks (KBr, cm^{-1}): *v* 3412, 3063, 1596, 1525, 1462, 1389, 1249, 699. ^{1}H NMR (400 MHz, DMSO) *δ* 13.00 (s, 2H), 8.03 (s, 2H), 7.67 (s, 2H), 7.34 (d, J = 10.4 Hz, 10H), 7.02 (d, J = 7.0 Hz, 6H), 6.89 (s, 4H). ^{13}C NMR (101 MHz, DMSO) *δ* 158.25, 136.14, 135.98, 133.72, 133.31, 129.63, 129.28, 128.90, 127.48, 122.79, 118.37, 116.62, 58.23. Anal. Calcd for $C_{42}H_{26}N_4O_2Br_4Zn$: C, 50.25; H, 2.59; N, 5.58%. Found: C, 50.29; H, 2.54; N, 5.59%.

C_4 (bis(2,4-diiodo-6-(4,5-diphenyl-1H-imidazol-2-yl)phenoxy)zinc): 92% yield. Mp. 280 – 281 °C. Selected IR peaks (KBr, cm^{-1}): *v* 3418, 1594, 1505, 1455, 1390, 1251, 696. ^{1}H NMR (400 MHz, DMSO) *δ* 12.97 (s, 2H), 8.12 (s, 2H), 7.93 (s, 2H), 7.34 (d, J = 6.2 Hz, 10H), 7.01 (d, J = 6.7 Hz, 6H), 6.87 (s, 4H). ^{13}C NMR (101 MHz, DMSO) *δ* 163.23, 145.86, 136.94, 137.63, 133.28, 129.49, 129.42, 128.84, 127.63, 127.49, 89.81, 89.58, 60.16. Anal. Calcd for $C_{42}H_{26}N_4O_2I_4Zn$•$COOCH_3$: C, 42.24; H, 2.32; N, 4.48%. Found: C, 42.25; H, 2.34; N, 4.50%.

C_5 (bis(4-methyl-2-(4,5-diphenyl-1H-imidazol-2-yl)phenoxy)zinc): 82% yield. Mp. 352 – 354 °C. Selected IR peaks (KBr, cm^{-1}): *v* 3052, 2920, 1598, 1494, 1444, 1305, 1242, 696. ^{1}H NMR (400 MHz, DMSO) *δ* 12.57 (s, 2H), 7.98 – 7.82 (m, 2H), 7.60 (s, 2H), 7.30 (m, 12H), 7.00 (m, 6H), 6.93 – 6.74 (m, 4H), 2.27 (d, J = 20.4 Hz, 4H), 1.84 (s, 2H). ^{13}C NMR (101 MHz, DMSO) *δ* 152.91, 135.22, 133.34, 131.96, 131.63, 130.12, 129.62, 129.43, 128.69, 127.67, 118.74, 116.83, 56.29, 25.31. Anal. Calcd for $C_{44}H_{34}N_4O_2Zn$: C, 73.85; H, 4.76; N, 7.83%. Found: C, 73.81; H, 4.77; N, 7.86%.

C_6 (bis(4-chloro-2-(4,5-diphenyl-1H-imidazol-2-yl)phenoxy)zinc): 93% yield. Mp. 362 – 364 °C. Selected IR peaks (KBr, cm^{-1}): *v* 3054, 1598, 1478, 1379, 1306, 1242, 696. ^{1}H NMR (400 MHz, DMSO) *δ* 12.77 (s, 2H), 7.87 (d, J = 2.9 Hz, 2H), 7.55 – 7.21 (m, 10H), 7.20 – 6.97 (m, 8H), 6.88 (t, J = 7.9 Hz, 4H), 6.74 (d, J = 9.0 Hz, 2H). ^{13}C NMR (101 MHz, DMSO) *δ* 152.37, 135.72, 132.04, 130.26, 129.78, 129.53, 128.98, 128.64, 128.30, 128.16, 120.31, 118.89, 56.49. Anal. Calcd for $C_{42}H_{28}N_4O_2Cl_2Zn$: C, 66.67; H, 3.70; N, 7.41%. Found: C, 66.70; H, 3.72; N, 7.45%.

C_7 (bis(4-bromo-2-(4,5-diphenyl-1H-imidazol-2-yl)phenoxy)zinc): 86% yield. Mp. 383 – 385 °C. Selected IR peaks (KBr, cm^{-1}): ν 3054, 2370, 1598, 1478, 1376, 1306, 1242, 697. ^{1}H NMR (400 MHz, DMSO) *δ* 12.78 (s, 2H), 7.98 (s, 2H), 7.59 – 7.16 (m, 12H), 7.04 (m, 6H), 6.89 (t, J = 7.7 Hz, 4H), 6.70 (d, J = 9.1 Hz, 2H). ^{13}C NMR (101 MHz, DMSO) *δ* 154.93, 137.63, 134.68, 133.27, 133.19, 128.99, 128.67, 128.31, 128.17, 120.97, 118.54, 104.20, 55.94. Anal. Calcd for $C_{42}H_{28}N_4O_2Br_2Zn$: C, 59.64; H, 3.31; N, 6.63%. Found: C, 59.61; H, 3.34; N, 6.62%.

C_8 (bis(4-nitro-2-(4,5-diphenyl-1H-imidazol-2-yl)phenoxy)zinc): 93% yield. Mp. 399 – 401 °C. Selected IR peaks (KBr, cm^{-1}): *v* 3245, 1604, 1563, 1484, 1306, 1133, 693. ^{1}H NMR (400 MHz, DMSO) *δ* 13.35 (s, 2H), 8.94 (s, 2H), 8.07 (s, 2H), 7.35 (d, J = 18.8 Hz, 10H), 6.98 (d, J = 20.9 Hz, 6H), 6.93 (d, 4H), 6.84 – 6.79 (m, 2H). ^{13}C NMR (101 MHz, DMSO) *δ* 162.04, 141.77, 136.76, 133.12, 129.73, 129.34, 128.74, 127.89, 123.86, 122.75, 119.84, 117.43, 59.88. Anal. Calcd for $C_{42}H_{28}N_6O_6Zn$: C, 64.86; H, 3.60; N, 10.81%. Found: C, 64.84; H, 3.61; N, 10.86%.

C_9 (bis(5-methoxy-2-(4,5-diphenyl-1H-imidazol-2-yl)phenoxy)zinc): 88% yield. Mp. 356 – 358 °C. Selected IR peaks (KBr, cm^{-1}): *v* 3226, 3053, 1606, 1546, 1447, 1322, 1155, 696. ^{1}H NMR (400 MHz, DMSO) *δ* 12.43 (s, 2H), 7.69 (d, J = 8.8 Hz, 2H), 7.31 (m, 10H), 7.04 (m, 6H), 6.88 (t, J = 7.6 Hz, 4H), 6.27 (d, J = 2.7 Hz, 2H), 6.23 – 6.15 (m, 2H), 3.75 (s, 6H). ^{13}C NMR (101 MHz, DMSO) *δ* 168.40, 162.47, 148.89, 133.58, 129.69, 128.95, 128.69, 128.32, 128.08, 127.49, 126.23, 106.74, 102.30, 55.13. Anal. Calcd for $C_{44}H_{34}N_4O_4Zn$: C, 70.68; H, 4.55; N, 7.50%. Found: C, 70.66; H, 4.54; N, 7.51%.

C_{10} (bis(2-(4,5-diphenyl-1H-imidazol-2-yl)phenoxy)copper): 99% yield. Mp. 226 – 228 °C. Selected IR peaks (KBr, cm^{-1}): *v* 3410, 3057, 1604, 1540, 1480, 1315, 1142, 696. A resolvable NMR spectrum could not be measured owing to paramagnetism.[45] Anal. Calcd for $C_{42}H_{30}N_4O_2Cu$•CH_3CH_2OH: C, 72.18; H, 4.92; N, 7.66%. Found: C, 72.17; H, 4.89; N, 7.68%.

C_{11} (bis(2-(4,5-diphenyl-1H-imidazol-2-yl)phenoxy)lead): 49% yield. Mp. 234 – 236 °C. Selected IR peaks (KBr, cm^{-1}): *v* 3418, 3060, 1600, 1528, 1482, 1245, 1139, 699. A resolvable NMR spectrum could not be measured owing to paramagnetism.[46] Anal. Calcd for $C_{21}H_{15}ON_2Pb$•$2COOCH_3$: C, 47.17; H, 3.30; N, 4.40%. Found: C, 47.18; H, 3.32; N, 4.41%.

C_{12} (bis(2-(4,5-diphenyl-1H-imidazol-2-yl)phenoxy)nickel): 12% yield (0.03 g). Mp. 360 – 363 °C. Selected IR peaks (KBr, cm^{-1}): *v* 3424, 3062, 1604, 1533, 1483, 1253, 1142, 696. A resolvable NMR spectrum could not be measured owing to paramagnetism.[47] Anal. Calcd for $C_{42}H_{30}N_4O_2Ni$•Cl•CH_3CH_2OH: C, 69.27; H, 4.72; N, 7.35%. Found: C, 69.27; H, 4.70; N, 7.37%.

C_{13} (bis(2-(4,5-diphenyl-1H-imidazol-2-yl)phenoxy)cobalt): 26% yield. Mp. 362 – 365 °C. Selected IR peaks (KBr, cm^{-1}): *v* 3412, 3060, 1604, 1533, 1482, 1243, 1143, 696. A resolvable NMR spectrum could not be measured owing to

View Article Online
DOI: 10.1039/C5RA08237D

paramagnetism.[48] Anal. Calcd for $C_{42}H_{30}N_4O_2Co{\bullet}Cl{\bullet}CH_3CH_2OH$: C, 69.25; H, 4.72; N, 7.34%. Found: C, 69.23; H, 4.73; N, 7.31%.

2.4. General procedure for the coupling reaction of epoxides and CO_2

A typical procedure for the coupling reaction of CO_2 and epoxide was as following (Scheme 2): A stainless steel autoclave (250 mL) was linked to CO_2 cylinders. A prescribed amount of epoxide was added with a hypodermic syringe. The catalysts were successively charged into the reactor without using any additional solvent. The reactor vessel was sealed and immersed into a oil bath at the desired temperature under stirring. Then, the CO_2 was pressurized into the reactor to the given pressure and the reaction started. After the given time, the reaction was stopped and the vessel was then cooled quickly by placing in an ice water and the pressure was released slowly. The result mixture was transferred to a 50 ml round bottom flask. The unreacted propylene oxide was removed in vacuo. The yield was calculated either by taking the weight of the result product or by comparing the ratio of the product to substrate peak areas obtained by ^1H NMR analysis. The selectivity of cyclic carbonate was determined by GC/MS (HP6890/5973). For all the experiments with different catalysts, no byproduct was detected.

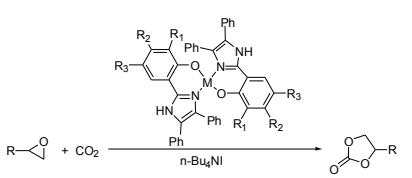

C_1: R_1 = H, R_2 = H, R_3 = H, M = Zn
C_2: R_1 = H, R_2 = H, R_3 = Cl, M = Zn
C_3: R_1 = H, R_2 = H, R_3 = Br, M = Zn
C_4: R_1 = H, R_2 = H, R_3 = I, M = Zn
C_5: R_1 = H, R_2 = H, R_3 = CH_3, M = Zn
C_6: R_1 = H, R_2 = H, R_3 = Cl, M = Zn
C_7: R_1 = H, R_2 = H, R_3 = Br, M = Zn
C_8: R_1 = H, R_2 = H, R_3 = NO_2, M = Zn
C_9: R_1 = H, R_2 = OCH_3, R_3 = H, M = Zn
C_{10}: R_1 = H, R_2 = H, R_3 = H, M = Cu
C_{11}: R_1 = H, R_2 = H, R_3 = H, M = Pb
C_{12}: R_1 = H, R_2 = H, R_3 = H, M = Ni
C_{13}: R_1 = H, R_2 = H, R_3 = H, M = Co

Scheme 2 Cycloaddition of PO and CO_2 to give PC and the metal catalysts C_1-C_{13} used in this study.

3. Results and discussion

3.1. X-ray crystallographic studies

The compounds C_1 and C_5 could be crystallized by slow evaporation of concentrate methanol solution. The formation of the complexes C_1 and C_5 was confirmed using single crystal X-ray crystallography (Fig. 1), and their crystallographic data, selected bond lengths and angles were reported in Table 1 and Table 2, respectively. The X-ray crystallographic characterizations have shown that each complex contains a zinc centre with a distorted tetrahedral N_2O_2-coordination sphere. The zinc centre of both complexes C_1 and C_5 possessed a cis-arrangement of the phenol O-donor atoms; i.e. the two 4,5-diphenyl imidazole units were accommodated on the same side of the complexes. The two ligands of each complex are related by a C_2-axis, but the two ligands are structurally inequivalent. Though the geometry at each zinc centre could be best described as a distorted tetrahedron in which two chelating ligands were placed in a similar disposition about the zinc centre, slight differences of the bond length and dihedral angle still occurred (Table 2), which indicated that in each complex, the orientation of the two ligands accommodated the normal geometrical preference of the zinc centre.[49-52]

3.2. Catalytic performances of C_1 with various additives

The activity of various additives was tested using the reaction of PO and CO_2 to produce PC, and the results are summarized in Table 3. Both the catalyst C_1 and the co-catalyst n-Bu_4NI could catalyze the cycloaddition alone, but the yields of PC were very low (entries 1, 2). As expected, the addition of moderate amounts of co-catalyst could greatly improve the yield of PC, TON value and TOF value (entry 3 vs 1, 2), especially for the quaternary ammonium salts. As for the quaternary ammonium salts (n-Bu_4NI, n-Bu_4NBr, and n-Bu_4NCl), the effect of halide anions I^-, Br^-, and Cl^- on the catalytic activity(entries 3-5) showed that the catalytic activity improved with the increase of leaving ability ($I^- > Br^- > Cl^-$).[53] Under the same condition, however, the activity decreased with other co-catalysts like Et_4NBr, PPh_3, DMAP and KI (entries 6-9). Therefore, n-Bu_4NI was selected as the co-catalyst to study the effect of reaction conditions on the coupling reaction in the presence of catalyst C_1.

Table 1 Crystallographic data for complexes C_1 and C_5

Identification code	$C_1{\cdot}3CH_3OH$	$C_5{\cdot}2CH_3OH$
Empirical formula	$C_{42}H_{30}N_4O_2Zn{\cdot}C_3H_{12}O_3$	$C_{44}H_{34}N_4O_2Zn{\cdot}C_2H_8O_2$
Formula weight (g mol^{-1})	784.20	780.21
Crystal size (mm^3)	0.12 × 0.10 × 0.10	0.12 × 0.10 × 0.10
Crystal system	Triclinic	Monoclinic
Space group	$P\bar{1}$	$C2/c$
Unit cell dimensions		
a (Å)	12.366(3)	28.552(3)
b (Å)	12.634(3)	13.6389(12)
c (Å)	14.695(4)	19.5849(18)
α (°)	67.273(3)	90
β (°)	67.681(4)	94.9510(10)
γ (°)	75.098(4)	90
Volume ($Å^3$)	1942.4(8)	7598.3(12)
Z	2	8
D_{calc} (g/cm^3)	1.341	1.364
σ (mm^{-1})	0.684	0.697
Collected refl.	36849	7972
Independent refl. (R_{int})	7490(0.0504)	10991(0.0787)
Parameters	502	502
$R_1[I > 2\sigma(I)]$	0.0779	0.0363
wR_2 (all data)	0.2323	0.1130
GOF	1.080	1.101

Table 2 Selected bond distances (Å) and angles (º) for compounds C_1 and C_5

	$C_1{\cdot}3CH_3OH$	$C_5{\cdot}2CH_3OH$
Bond distances (Å)		
Zn(1)-O(2)	1.944(2)	1.9375(9)
Zn(1)-O(1)	1.940(2)	1.9336(9)
Zn(1)-N(1)	1.972(3)	1.9925(11)
Zn(1)-N(3)	1.979(3)	1.9801(11)
Bond angles (°)		
O(2)-Zn(1)-O(1)	110.21(11)	116.94(4)
O(2)-Zn(1)-N(1)	121.40(11)	113.53(4)
O(1)-Zn(1)-N(1)	96.15(11)	96.06(4)
O(2)-Zn(1)-N(3)	94.63(10)	94.59(4)
O(1)-Zn(1)-N(3)	110.17(11)	115.46(4)
N(1)-Zn(1)-N(3)	124.40(11)	121.92(4)

View Article Online
DOI: 10.1039/C5RA08237D

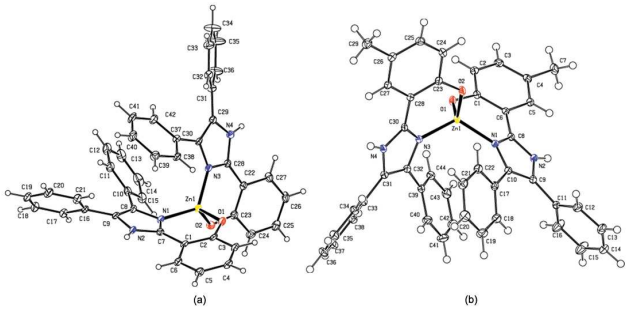

Fig. 1 ORTEP representations of the molecular structures of (a) complex C_1 and (b) complex C_5. Structural differences are caused by steric effects of substituentson the imidazole ring.

Table 3 Coupling of CO_2 and PO catalyzed by various components[a]

Entry	Catalyst	Yield (%)[b]	TON[c]	TOF (h^{-1})[d]
1	C_1	3.5	35.0	7.0
2	n-Bu_4NI	21.7	254.0	50.8
3	C_1/n-Bu_4NBr	91.4	914.0	182.8
4	C_1/n-Bu_4NCl	42.4	423.5	84.7
5	C_1/n-Bu_4NI	95.8	958.0	191.6
6	C_1/Et_4NBr	87.3	873.0	174.6
7	C_1/PPh_3	5.5	55.0	11.0
8	C_1/DMAP	12.6	125.5	25.1
9	C_1/KI	52.1	521.0	104.2

[a] Catalyst: 0.214 mmol; co-catalyst: 0.214 mmol; PO: 15 mL, 0.214 mol; CO_2 pressure: 5 MPa; time: 5 h; temperature: 130 °C, the selectivity to products are all > 99 %. [b] Isolated yields. [c] Turnover number for PC calculated as moles of PC produced per mole of catalyst. [d] Turnover frequency for PC calculated as mole of PC produced per mole of catalyst per hour.

3.3. The effect of reaction pressure

Generally, a significant disadvantage associated with CO_2 as reagent or reaction medium in organic synthesis is the potential dangers operated at high pressures.[24] Thus, the effect of CO_2 pressure on the catalytic activity was studied at 130 °C in pressure range of 1-7 MPa, and the results are shown in Fig. 2. PC yield increased dramatically with increasing pressure in the range of 1-2 MPa, then remained almost constant with further increase in pressure. The further CO_2 pressure increase beyond 2 MPa apparently favored a slightly increased PC formation, but the rise is unnecessary. This may be attributed to the phase behaviour of CO_2-PO system which resulted in the effect of pressure on the concentrations of CO_2 and PO.[54] There were three phases in the reaction system including the top CO_2-rich gas phase, catalyst-rich solid phase and the bottom PO-rich liquid phase. The reaction mostly took place in the PO–catalyst interface. The initial increase of CO_2 pressure (0–2 MPa) led to the increased concentration of CO_2 in the liquid phase, which is why the PC yield was raised significantly. Nevertheless, the PC yield no longer increased with the CO_2 pressure beyond 2 MPa up to 7 MPa. This may be due to the higher pressure extracted a certain amount of PO into the gas phase, and caused the decline of PO concentration in the vicinity of the catalyst in the liquid phase.[55] Besides, the instrument which is operated under high pressure condition is too expensive to afford in industry application. Therefore, 2 MPa was chosen as the optimal reaction pressure in the following catalytic reaction of CO_2 and PO to PC.

3.4. The effect of reaction time

The PC yield versus reaction time was shown in Fig. 3. The PC synthesis from PO and CO_2 proceeded rapidly, and nearly 80% PC yield was obtained within the first 3 h at 130 °C. The PC yield experienced a continuing growth within 5 h, and then gradually decreased. It is noted that a further increase in the reaction time led to a slight decrease in PC yield. This may be due to that the interaction between catalysts and reactant was obstructed by the formed PC.[56] The growing viscosity of the reaction system was also another negative factor for the activation of CO_2 at longer reaction time. The selectivity of PC stayed above 99% throughout. So, a reaction time of 5 h was required for further research.

3.5. The effect of reaction temperature

The effect of the temperature on the cycloaddition reaction catalyzed by C_1 in the presence of n-Bu_4NI in the temperature range of 50-130 °C was shown in Fig. 4. The figure illustrated that the activity of the catalyst was strongly affected by reaction temperature.[57] The yield of PC increased with increasing temperature, and reached 90.3% at 110 °C, then the PC yield only slightly increased with further increase of temperature, indicating that 110 °C was the optimal temperature. It is also interesting to note that no by-product polyether was detected even at very low temperature, which indicated that the catalyst used in this work had a good selectivity for the production of PC.[58]

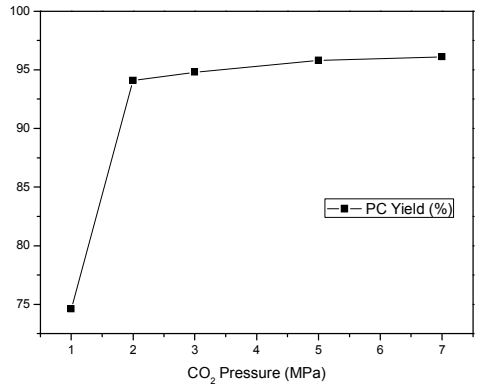

Fig. 2 Effect of CO_2 pressure on PC yield. Reaction conditions: 0.214 mmol C_1, 0.214 mmol n-Bu_4NI, 0.214 mol PO, reaction temperature 130 °C, reaction time 5 h, the selectivity to products are all > 99 %.

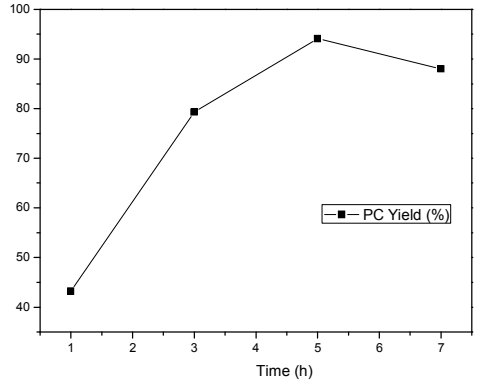

Fig. 3 Effect of reaction time on PC yield. Reaction conditions: 0.214 mmol C_1, 0.214 mmol n-Bu_4NI, 0.214 mol PO, reaction temperature 130 °C, CO_2 pressure 2 MPa, the selectivity to products are all > 99 %.

View Article Online
DOI: 10.1039/C5RA08237D

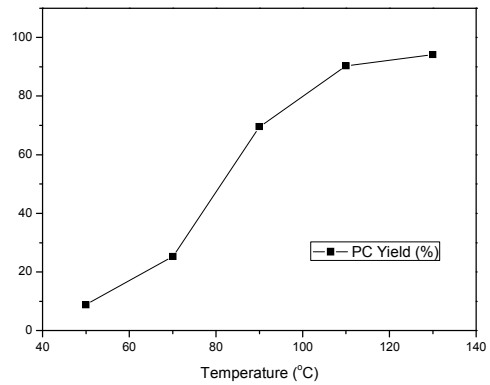

Fig. 4 Effect of reaction temperature on PC yield. Reaction conditions: 0.214 mmol C_1, 0.214 mmol n-Bu_4NI, 0.214 mol PO, reaction time 5 h, CO_2 pressure 2 MPa, the selectivity to products are all > 99 %.

3.6. Effect of substitution on the aromatic rings of Complexes

The substitution on the aromatic rings of salicylaldehyde probably causes geometrical distortion of space structure, and thus, may affect properties of catalyst. So, the effect of substitution on the aromatic rings of complexes was investigated. The experimental results in Table 4 showed that although this series of catalysts had good catalytic performance under optimal conditions (110 °C, 5 h, 2 MPa), the catalytic activity of these catalysts exhibited some difference for different substitutions. Under the same conditions, catalytic activities of 3,5-substituted complexes were in the following order: C_4 (-I) (95.9%) > C_3 (-Br) (94.2%) > C_2 (-Cl) (94.0%) > C_1 (-H) (90.3%), which indicated that the electron-withdrawing effect played a key role in the decrease of catalytic property of these zinc complexes.[59,60] For the 5-substituted Zn complexes, the order was: C_7 (-Br) (99.7%) > C_6 (-Cl) (94.6%)> C_8 (-NO_2) (94.1%) > C_5 (-CH_3) (89.3%), while the order of electron-withdrawing effect was: -NO_2 > -Cl > -Br > -CH_3. The exception of C_5 (-CH_3) might be attributed to the steric hindrance effect of methyl, which was not benefit for the insertion of propylene oxide into the metal centre.[61] Ko and co-workers had reported homologous zinc catalysts bearing iminebenzotriazole phenoxide ligands,[62] which were active catalyst(TOF: 33.3 h^{-1}) for the cycloaddition of CO_2 with propylene oxide in the presence of n-Bu_4NBr to give propylene carbonate (PC) under mild conditions (table 4, entry 10). Both Ko's and present works proved that zinc complexes with phenoxide ligands possessed excellent catalytic performance for the coupling reaction of CO_2 and epoxide.

Table 4 Effect of substitution on the aromatic rings on the catalytic activity[a]

Entry	Catalyst	Yield (%)[b]	TON[c]	TOF (h^{-1})[d]
1	C_1/n-Bu_4NI	90.3	903.0	180.6
2	C_2/n-Bu_4NI	94.0	940.0	188.0
3	C_3/n-Bu_4NI	94.2	942.0	188.4
4	C_4/n-Bu_4NI	95.9	959.0	191.8
5	C_5/n-Bu_4NI	89.3	893.0	178.6
6	C_6/n-Bu_4NI	94.6	946.0	189.2
7	C_7/n-Bu_4NI	99.7	997.0	199.4
8	C_8/n-Bu_4NI	94.1	941.0	188.2
9	C_9/n-Bu_4NI	90.2	902.0	180.4
10[e]	(^{C8Fu}IBTP)$_2$Zn /n-Bu_4NI	37.0	370.0	15.4
12	C_{10}/n-Bu_4NI	56.2	562.0	112.4
13	C_{11}/n-Bu_4NI	80.1	801.0	160.2
14	C_{12}/n-Bu_4NI	81.2	812.0	162.4
15	C_{13}/n-Bu_4NI	91.1	911.0	182.2

[a] Catalyst: 0.214 mmol; n-Bu_4NI: 0.214 mmol; PO: 15 mL, 0.214 mol; CO_2 pressure: 2 MPa; time: 5 h; temperature: 110 °C, the selectivity to products are all > 99 %. [b] Isolated yields. [c] Turnover number for PC calculated as moles of PC produced per mole of catalyst. [d] Turnover frequency for PC calculated as mole of PC produced per mole of catalyst per hour. [e] Ref. 62: Catalyst (mol%): 0.1, PO: 5.0 mL, 50 °C, 1.0 MPa initial CO_2 pressure, 24 h.

3.7. Effect of central metal on the activity

In order to make a systematic comparison, the catalytic properties of C_{10} (Cu), C_{11} (Pb), C_{12} (Ni), and C_{13} (Co) were also investigated (Table 4). Except Cu centre, the PC yield catalyzed by other four metal centre complexes (Zn, Pb, Ni, Co) were all > 80%, and the activity order was C_{13} (Co) (91.1%) > C_1 (Zn) (90.3%) > C_{12} (Ni) (81.2%) > C_{11} (Pb) (80.1%) > C_{10} (Cu) (56.2%), which indicated that the catalytic activity is highly dependent on the type of centre metal. It is possible that the high catalytic activities of the cobalt(II)-, zinc(II)-, nickel(II)-, lead(II)-centre complexes and the low activity of the copper(II)- centre complexes are related to the metal's different coordination ability with PO.[63,64] It's worthily noted that most Pb or Pb(II) compounds were used as electrodes for the electrochemical reduction of CO_2.[65] The present study is the first report about the usefulness of lead catalyst for coupling reaction between CO_2 and epoxides.

3.8. Catalyst recycling

As well-known, the stability and reusability of a catalyst are two key factors for practical application in industry. Catalyst C_1 was chosen to evaluate the recyclability, and then a series of catalytic cycles for the coupling reaction of CO_2 with PO was carried out under the optimized reaction conditions (110 °C, 5 h, 2 MPa). In each cycle, the catalyst C_1 could be easily separated from the product by the addition of ethanol, subsequent filtration and then used for the next run directly. The results in Fig. 5 exhibited that the catalyst C_1 could be reusable for at least 5 times without significant loss of activity, while the selectivity of the product remained the same.

View Article Online
DOI: 10.1039/C5RA08237D

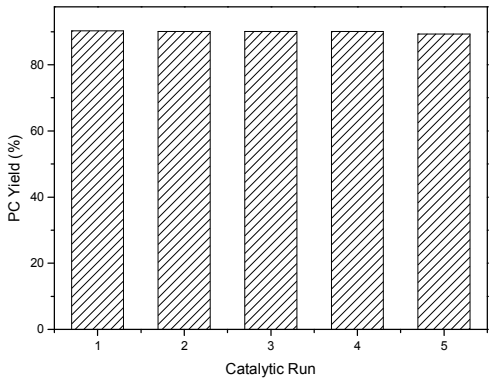

Fig. 5 Catalyst recycling with 0.214 mmol C_1/0.214 mmol n-Bu_4NI/0.214 mol PO at 110 °C, 2 MPa CO_2, and 5 h (>99 % PC selectivity is maintained).

3.9. Applicability of substrates

The catalytical performance of C_1/n-Bu_4NI for the cycloaddition of CO_2 with other epoxides were also studied at 110 °C, 5 h and 2 MPa without any organic solvent, and the results are summarized in Table 5. The catalyst was applicable to a variety of terminal epoxides to produce the corresponding cyclic carbonates with excellent yields, with the exception of isobutylene oxide (entry 5) and cyclohexene oxide (entry 6), which was probably due to their higher steric hindrance.[66,67] This steric effect was more likely to hinder the nucleophilic attack of the epoxide rather than its coordination to the Lewis acid metal centre.[68,69]

Table 5 Cycloaddition between CO_2 and various epoxides catalyzed by C_1 in the presence of n-Bu_4NI[a]

Entry	Epoxide	Product	Yield (%)[b]	TON[c]	TOF (h^{-1})[d]
1	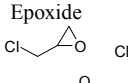	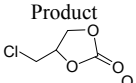	98.1	981.0	196.2
2	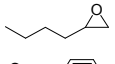	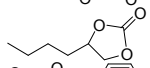	93.8	938.0	187.6
3	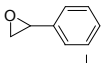	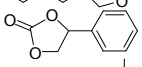	93.1	931.0	186.2
4	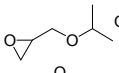	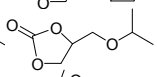	93.4	934.0	186.8
5		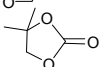	19.3	193.0	38.6
6		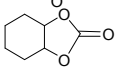	42.6	426.0	85.2

[a] C_1: 0.214 mmol; n-Bu_4NI: 0.214 mmol; epoxide: 0.214 mol; CO_2 pressure: 2 MPa; time: 5 h; temperature: 110 °C, the selectivity to products are all > 99 %. [b] Isolated yields. [c] Turnover number for carbonates calculated as moles of carbonate produced per mole of catalyst. [d] Turnover frequency for carbonates calculated as mole of carbonate produced per mole of catalyst per hour.

3.10. Proposed mechanism of the coupling reaction

The metal-catalyzed coupling reaction of CO_2 and epoxides is generally thought to occur via a coordination-insertion mechanism.[70] Taking into account the diverse mechanisms found in the literature for the coupling of epoxide and CO_2[71-74] and DFT studies involving in particular zinc salphen,[69] a general mechanism can be illustrated for the M–N_2O_2/(n-Bu)$_4$NX catalytic system in Scheme 3. Considering that the reports on ionic metal salens of the type [N_2O_2M-X][NR_4] have been scarce, a neutral M–N_2O_2 species as the starting point in the catalytic cycle.[40] The ligands of the catalysts comprise a N_2O_2 coordination pocket into which a wide variety of metal ions can be easily accommodated and that function as the catalytic center. Various substituents can be easily introduced in the aromatic rings to allow, for example, control over the approach of a substrate by bulky groups or variation of the Lewis acidity of the metal center through electron-withdrawing/donating groups. The insertion of appropriate substituents on the phenyl ring can also be employed to anchor the salen scaffold to a solid support, thus allowing for the preparation of heterogeneous catalysts.[75] The epoxide ring of PO was activated by M–N_2O_2 species, and then the epoxide ring was attacked by the anion of co-catalyst such as n-Bu_4NI, leading to epoxide ring-opening and formation of a metal-bound alkoxide. At the same time, CO_2 inserted into the metal–alkoxide bond to form a metal alkylcarbonate, and then the production of cyclic carbonate was formed via a backbiting pathway.[76] This mechanism indicated that the presence of a nucleophilic group, either a nucleophilic axial anion or an added co-catalyst, and a metal centre were both necessary for the reaction, that is why the PC yield was very low when catalyzed by the metal complex C_1 or co-catalyst n-Bu_4NI alone (Table 4, entries 1 and 2).

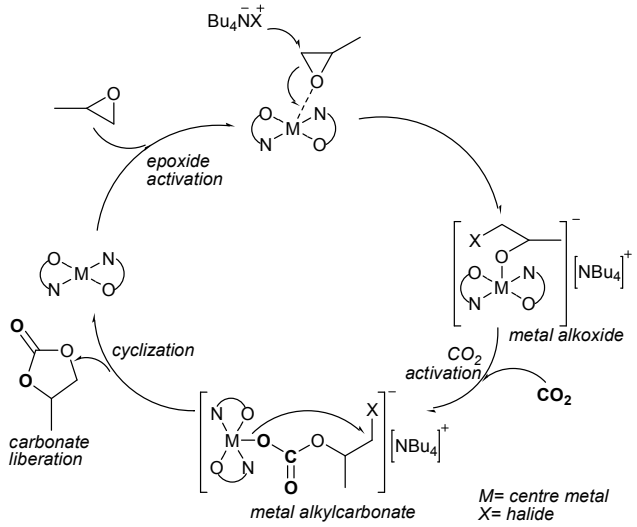

Scheme 3 Proposed mechanism for cyclic carbonate formation.

Conclusions

In summary, a series of easily accessible metal complexes bearing 2-(imidazol-2-yl)phenol ligands were synthesized and characterized. Systematical investigation demonstrated that all the complexes were active and versatile catalysts for the coupling reaction of CO_2 and epoxides to selectively generate cyclic carbonate without any organic solvents. The effect of reaction conditions (time, temperature and pressure), substitution on the aromatic rings of ligands and central metal on the catalytic activity were investigated, and the optimal catalytical conditions were screened as 110 °C, 5 h, 2 MPa. The catalyst also could be reused several times with only minor loss in the catalyst activity. This catalyst system was also suitable for the production of cyclic carbonates from CO_2 and epoxides. These characteristics made them ideal catalysts in terms of potential industrial application in chemical CO_2 fixation.

View Article Online
DOI: 10.1039/C5RA08237D

Acknowledgements

We are grateful to National Natural Science Foundation of China (No. 51073175).

Abbreviations

CO_2, carbon dioxide; PO, propylene oxide; PC, propylene carbonate; MOFs, metal–organic frameworks; CaH_2, calcium hydride; TMS, trimethylsilane; CH_2Cl_2, dichloromethane; $MgSO_4$, magnesium sulfate anhydrous; DMSO, dimethylsulfoxide; DMAP, 4-dimethylaminopyridine; KI, potassium iodide; PPh_3, triphenylphosphine; n-Bu_4NBr, tetrabutylammonium bromide; n-Bu_4NCl, tetrabutylammonium chloride; n-Bu_4NI, tetrabutylammonium iodide.

Notes and references

[a]*The State Key Laboratory of Power Transmission Equipment & System Security and New Technology, College of Chemistry and Chemical Engineering, Chongqing university, Chongqing 400044, China*
[b]*Key Laboratory of Catalysis and Materials Science of the State Ethnic Affairs Commission & Ministry of Education, Hubei Province, Key Laboratory of Analytical Chemistry of the State Ethnic Affairs Commission, College of Chemistry and Materials Science, South-Central University for Nationalities, Wuhan, 430074, P.R. China. Tel./Fax: +86-27-67842752; Email addresses: yanghaijian@vip.sina.com*
[c]*School of Chemistry and Chemical Engineering, University of Chinese Academy of Sciences, Beijing, 100049, P.R. China*
Email addresses:cyguo@ucas.ac.cn

† Electronic Supplementary Information (ESI) available: [details of any supplementary information available should be included here]. See DOI: 10.1039/b000000x/

1 I. Omae, Catal. Today, 2006, **115**, 33.
2 T. Sakakura, J. C. Choi, H. Yasuda, *Chem. Rev*., 2007, **107**, 2365.
3 A. T. Najafabadi, *Int. J. Energy Res.*, 2013, **37**, 485.
4 T. Sakakura, K. Kohno, *Chem. Commun.*, 2009, 1312.
5 J. Sebastian, S. Darbha, *RSC Adv.*, 2015, **5**, 18196.
6 D. J. Darensbourg, W. C. Chung, K. Wang, H. C. Zhou, *ACS Catal.*, 2014, **4**, 1511−1515.
7 R. J. Wei, X. H. Zhang, Y. Y. Zhang, B. Y. Du, Z. Q. Fan, G. R. Qi, *RSC Adv.*, 2014, **4**, 3188.
8 I. S. Metcalfe, M. North, P. J. Villuendas, *J. CO_2 Utilization*, 2013, **2**, 24.
9 Y. Xie, T. T. Wang, X. H. Liu, K. Zou, W. Q. Deng, *Nat. Commun.*, 2013, **4**, 1.
10 Z. Zhang, L. Xu, W. Feng, *RSC Adv.*, 2015, **5**, 12382.
11 J. A. Castro-Osma, C. Alonso-Moreno, A. Lara-Sánchez, J. Martínez, M. North, A. Otero, *Catal. Sci. Technol.*, 2014, **4**, 1674.
12 S. H. Li, B. Miao, W. M. Yuan, S. M. Ma, *Org. Lett.*, 2013, **15**, 977.
13 X. D. Tang, C. R. Qi, H. T. He, H. F. Jiang, Y. W. Ren, G. Q. Yuan, *Adv. Synth. Catal.*, 2013, **355**, 2019.
14 J. C. Choi, K. Shiraishi, Y. Takenaka, H. Yasuda, T. Sakakura, *Organometallics*, 2013, **32**, 3411.
15 Y. Chen, R. Qiu, X. Xu, C. T. Au, S. F. Yin, *RSC Adv.*, 2014, **4**, 11907.
16 N. M. Rajendran, A. Haleel, N. D. Reddy, *Organometallics*, 2014, **33**, 217.
17 T. Ema, Y. Miyazaki, S. Koyama, Y. Yano, T. Sakai, *Chem. Commun.*, 2012, **48**, 4489.
18 J. Meléndez, M. North, P. Villuendas, *Chem. Commun.*, 2009, 2577.
19 H. Y. Ju, M. D. Manju, K. H. Kim, S. W. Park, D. W. Park, *J. Ind. Eng. Chem.*, 2008, **14**, 157.
20 W. L. Dai, B. Jin, S. L. Luo, X. B. Luo, X. M. Tu, C. T. Au, *Catal. Sci. Technol.*, 2014, **4**, 556.
21 W. L. Wong, L. Y. S. Lee, K. P. Ho, Z. Y. Zhou, T. Fan, Z. Y. Lin, K. Y. Wong, *Appl. Catal. A*, 2014, **472**, 160.
22 A. Ion, V. Parvulescu, P. Jacobs, D. de Vos, *Appl. Catal. A*, 2009, **363**, 40.
23 J. Tharun, K. R. Roshan, A. C. Kathalikkattil, D. H. Kang, H. M. Ryu, D. W. Park, *RSC Adv.*, 2014, **4**, 41266.
24 M. Liu, B. Liu, L. Shi, F. Wang, L. Liang, J. Sun, *RSC Adv.*, 2015, **5**, 960.
25 J. Peng, H. J. Yang, N. Song, C. Y. Guo, *J. CO_2 Util.*, 2015, **9**, 16.
26 W. L. Dai, S. L. Luo, S. F. Yin, C. T. Au, *Appl. Catal. A*, 2009, **366**, 2.
27 M. Aresta, A. Dibenedetto, L. Gianfrate, C. Pastore, *Appl. Catal. A*, 2003, **25**, 5.
28 Q. W. Song, L. N. He, J. Q. Wang, H. Yasuda, T. Sakakura, *Green Chem.*, 2013, **15**, 110.
29 A. Siewniak, K. Jasiak, S. Baj, *Appl. Catal. A*, 2014, **482**, 266.
30 J. X. Chen, B. Jin, W. L. Dai, S. L. Deng, L. R. Cao, Z. J. Cao, S. L. Luo, X. B. Luo, X. M. Tu, C. T. Au, *Appl. Catal. A*, 2014, **484**, 26.
31 H. Li, P. S. Bhadury, B. Song, S. Yang, *RSC Adv.*, 2012, **2**, 12525.
32 S. D. Lee, B. M. Kim, D. W. Kim, M. I. Kim, K. R. Roshan, M. K. Kim, Y. S. Won, D. W. Park, *Appl. Catal. A*, 2014, **486**, 69.
33 J. Q. Wang, W. G. Cheng, J. Sun, T. Y. Shi, X. P. Zhang, S. J. Zhang, *RSC Adv.*, 2014, **4**, 2360.
34 D. Srinivas, P. Ratnasamy, *Micropor. Mesopor. Mater.*, 2007, **105**, 170.
35 R. Srivastava, D. Srinivas, P. Ratnasamy, *Appl. Catal. A*, 2005, **289**, 128.
36 Y. Ren, Y. Shi, J. Chen, S. Yang, C. Qi, H. Jiang, *RSC Adv.*, 2013, **3**, 2167.
37 H. Y. Cho, D. A. Yang, J. S. Kim, Y. Jeong, W. S. Ahn, *Catal. Today*, 2012, **185**, 35.
38 J. Kim, S. N. Kim, H. G. Jang, G. Seo, W. S. Ahn, *Appl. Catal. A*, 2013, **453**, 175.
39 M. A. Fuchs, S. Staudt, C. Altesleben, O. Walter, T. A. Zevaco, E. Dinjus, *Dalton Trans.*, 2014, **43**, 2344.
40 M. A. Fuchs, C. Altesleben, S. C. Staudt, O. Walter, T. A. Zevaco, E. Dinjus, *Catal. Sci. Technol.*, 2014, **4**, 1658.
41 A. Decortes, A. W. Kleij, *ChemCatChem*, 2011, **3**, 831.
42 M. Taherimehr, A. Decortes, S. M. Al-Amsyar, W. Lueangchaichaweng, C. J. Whiteoak, E. C. Escudero-Adán, A. W. Kleij, P. P. Pescarmona, *Catal. Sci. Technol.*, 2012, **2**, 2231.
43 A. Decortes, M. M. Belmonte, J. Benet-Buchholz, A. W. Kleij, *Chem. Commun.*, 2010, **46**, 4580.
44 A. O. Eseola, W. Li, R. Gao, M. Zhang, X. Hao, T. L. Liang, N. O. Obi-Egbedi, W. H. Sun, *Inorg. Chem.*, 2009, **48**, 9133.
45 S. López-Rayo, J. J. Lucena, *J. Agric. Food Chem.*, 2011, **59**, 13110.
46 V. K. Koltover, J. W. Logan, H. Heise, V. P. Bubnov, Y. I. Estrin, I. E. Kareev, V. P. Lodygina, A. Pines, *J. Phys. Chem. B*, 2004, **108**, 12450.
47 P. Chaudhuri, C. N. Verani, E. Bill, E. Bothe, T. Weyhermüller, K. Wieghardt, *J. Am. Chem. Soc.*, 2001, **123**, 2213.
48 M. J. Knight, I. C. Felli, R. Pierattelli, L. Emsley, G. Pintacuda, *Acc. Chem. Res.*, 2013, **46**, 2108.
49 L. Benisvy, A. J. Blake, D. Collison, E. S. Davies, C. D. Garner, E. J. L. Mclnnes, J. McMaster, G. Whittaker, C. Wilson, *Chem. Commun.*, 2001, 1824.
50 L. Benisvy, A. J. Blake, D. Collison, E. S. Davies, C. D. Garner, E. J. L. Mclnnes, J. McMaster, G. Whittaker, C. Wilson, *Dalton Trans.*, 2003, 1975.
51 L. Benisvy, E. Bill, A. J. Blake, D. Collison, E. S. Davies, C. D. Garner, C. I. Guindy, E. J. L. Mclnnes, G. McArdle, J. McMaster, C. Wilson, J. Wolowska, *Dalton Trans.*, 2004, 3647.
52 L. Benisvy, E. Bill, A. J. Blake, D. Collison, E. S. Davies, C. D. Garner, G. McArdle, E. J. L. Mclnnes, J. McMaster, S. H. K. Ross, C. Wilson, *Dalton Trans.*, 2006, 258.
53 Z. F. Yang, J. Sun, W. G. Cheng, J. Q. Wang, Q. Li, S. J. Zhang, *Catal. Commun.*, 2014, **44**, 6.
54 Y. Y. Zhang, S. F. Yin, S. L. Luo, C. T. Au, *Ind. Eng. Chem. Res.*, 2012, **51**, 3951.
55 W. L. Dai, B. Jin, S. L. Luo, X. B. Luo, X. M. Tu, C. T. Au, *J. Mol. Catal. A*, 2013, **378**, 326.

View Article Online
DOI: 10.1039/C5RA08237D

56 D. S. Bai, H. W. Jing, G. J. Wang, *Appl. Organometal. Chem.*, 2012, **26**, 600.
57 J. L. Song, B. B. Zhang, P. Zhang, J. Ma, J. L. Liu, H. L. Fan, T. Jiang, B. X. Han, *Catal. Today*, 2012, **183**, 130.
58 O. V. Zalomaeva, A. M. Chibiryaev, K. A. Kovalenko, O. A. Kholdeeva, B. S. Balzhinimaev, V. P. Fedin, *J. Catal.*, 2013, **298**, 179.
59 L. Dai, X. Li, H. Yuan, X. Li, Z. H. Li, D. Xu, F. Fei, Y. Q. Liu, J. Zhang, Z. M. Zhou, *Tetrahedron: Asymmetry*, 2011, **22**, 1379.
60 Y. Sun, W. S. Zhang, X. B. Hu, H. R. Li, *J. Phys. Chem. B*, 2010, **114**, 4862.
61 X. B. Lu, X. J. Feng, R. He, *Appl. Catal. A*, 2002, **234**, 25.
62 T. Y. Chen, C. Y. Li, C. Y. Tsai, C. H. Li, C. H. Chang, B. T. Ko, C. Y. Chang, C. H. Lin, H. Y. Huang, *J. Organomet. Chem.*, 2014, **754**, 16. (Table 3, entry 3)
63 S. H. Szczepankiewicz, C. M. Ippolito, B. P. Santora, T. J. Van de Ven, G. A. Ippolito, L. Fronckowiak, F. Wiatrowski, T. Power, M. Kozik, *Inorg. Chem.*, 1998, **37**, 4344.
64 H. Yasuda, L. N. He, T. Sakakura, C. Hu, *J. Catal.*, 2005, **233**, 119.
65 J. Qiao, Y. Liu, F. Hong, J. Zhang, *Chem. Soc. Rev.*, 2014, **43**, 631.
66 C. J. Whiteoak, N. Kielland, V. Laserna, E. C. Escudero-Adán, E. Martin, A. W. Kleij, *J. Am. Chem. Soc.*, 2013, **135**, 1228.
67 J. Tharun, G. Mathai, R. Roshan, A. C. Kathalikkattil, K. Bomi, D. W. Park, *Phys. Chem. Chem. Phys.*, 2013, **15**, 9029.
68 C. Martín, C. J. Whiteoak, E. Martin, B. M. Martínez, E. C. Escudero-Adán, A. W. Kleij, *Catal. Sci. Technol.*, 2014, **4**, 1615.
69 F. Castro-Gómez, G. Salassa, A. W. Kleij, C. Bo, *Chem. Eur. J.*, 2013, **19**, 6289.
70 S. Supasitmongkol, P. Styring, *Catal. Sci. Technol.*, 2014, **4**, 1622.
71 M. North, R. Pasqualem C. Young, *Green Chem.*, 2010, **12**, 1514.
72 M. R. Kember, A. Buchard, C. K. Williams, *Chem. Commun.*, 2011, **47**, 141.
73 M. Cokoja, C. Bruckmeier, B. Rieger, W. A. Herrmann, F. E. Kühn, *Angew. Chem., Int. Ed.*, 2011, **50**, 8510.
74 P. P. Pescarmonam M. Taherimehr, *Catal. Sci. Technol.*, 2012, **2**, 2169.
75 A. Decortes, A. M. Castilla, A. W. Kleij, *Angew. Chem., Int. Ed.* 2010, **49**, 9822.
76 A. C. Kathalikkattil, R. Roshan, J. Tharun, H. G. Soek, H. S. Ryu, D. W. Park, *ChemCatChem*, 2014, **6**, 284.